Ovarian Dendritic Cells Act as a Double-Edged Pro-Ovulatory and Anti-Inflammatory Sword

Adva Cohen-Fredarow,* Ari Tadmor,* Tal Raz,* Naama Meterani, Yoseph Addadi, Nava Nevo, Inna Solomonov, Irit Sagi, Gil Mor, Michal Neeman, and Nava Dekel

Department of Biological Regulation (A.C.-F., A.T., N.M., Y.A., N.N., I.So., I.Sa., M.N., N.D.), Weizmann Institute of Science, Rehovot 76100, Israel; Koret School of Veterinary Medicine (T.R.), The Hebrew University of Jerusalem, Rehovot 76100, Israel; B-nano Ltd (Y.A.), Rehovot 76326, Israel; and Department of Obstetrics Gynecology and Reproductive Science (G.M.), Reproductive Immunology Unit, Yale University School of Medicine, New Haven, Connecticut 06510

Ovulation and inflammation share common attributes, including immune cell invasion into the ovary. The present study aims at deciphering the role of dendritic cells (DCs) in ovulation and corpus luteum formation. Using a CD11c-EYFP transgenic mouse model, ovarian transplantation experiments, and fluorescence-activated cell sorting analyses, we demonstrate that CD11c-positive, F4/80-negative cells, representing DCs, are recruited to the ovary under gonadotropin regulation. By conditional ablation of these cells in CD11c-DTR transgenic mice, we revealed that they are essential for expansion of the cumulus-oocyte complex, release of the ovum from the ovarian follicle, formation of a functional corpus luteum, and enhanced lymphangiogenesis. These experiments were complemented by allogeneic DC transplantation after conditional ablation of CD11c-positive cells that rescued ovulation. The pro-ovulatory effects of these cells were mediated by up-regulation of ovulation-essential genes. Interestingly, we detected a remarkable anti-inflammatory capacity of ovarian DCs, which seemingly serves to restrict the ovulatory-associated inflammation. In addition to discovering the role of DCs in ovulation, this study implies the extended capabilities of these cells, beyond their classic immunologic role, which is relevant also to other biological systems. **(*Molecular Endocrinology* 28: 1039–1054, 2014)**

The analogy between inflammation and ovulation, first suggested 3 decades ago (1), took into account ovarian attributes associated with an immune response, such as increased vascular permeability and prostaglandin synthesis. Moreover, expression levels of inflammation-associated genes such as cyclooxygenase-2 (*Ptgs2*), hyaluronan synthase-2 (*Has2*), and TNFα-stimulated gene-6 (*Tnfaip6*) are up-regulated in the ovary in response to the preovulatory surge of LH (2). Finally, follicle rupture, which allows the release of the ovum from the ovarian follicle, involves the action of proteinases, bradykinins, and histamine, accompanied by enhanced ovarian blood flow, all attributes of acute inflammatory reaction (3–8). Similarly, accumulating evidence suggests that different leukocyte populations are recruited to the ovary under gonadotropin regulation. Specifically, localization and characterization of ovarian leukocyte subsets, such as macrophages, mast cells, neutrophils, T lymphocytes, and more recently CD8$\alpha^{+/+}$ cells, are currently established, although the role these cells play during ovulation is only partially documented (9–12). On the other hand, the potential role of CD11c-positive, F4/80-negative cells, apparently representing dendritic cells (DCs), in ovulation has not been studied.

ISSN Print 0888-8809 ISSN Online 1944-9917
Printed in U.S.A.

Received November 25, 2013. Accepted April 30, 2014.
First Published Online May 13, 2014

* A.C.-F., A.T., and T.R. contributed equally to the study.

Abbreviations: 7AAD, 7-aminoactinomycin D; COC, cumulus-oocyte complex; DC, dendritic cell; DTR, diphtheria toxin receptor; DTX, diphtheria toxin; EYFP, enhanced yellow fluorescent protein; FACS, fluorescence-activated cell sorting; GFP, green fluorescent protein; hCG, human chorionic gonadotropin; LYVE-1, lymphatic vessel endothelial receptor 1; MHCII, major histocompatability complex class II; PMSG, pregnant mare serum gonadotropin; SMA, smooth muscle actin; STAR, steroidogenic acute regulatory protein; TNFAIP6, TNFα-stimulated gene-6.

DCs are specialized antigen-presenting cells, which play a pivotal role in initiating and coordinating the innate and adaptive immune responses by priming T cells (13–15). An increasing body of evidence suggests that aside from the classic role of DCs in inducing immunity against infectious agents, they also take part in the immune tolerance to innocuous antigens (16, 17). More recent studies employed conditional ablation of CD11c-positive cells by using the CD11c-diphtheria toxin receptor (DTR) transgenic mice, in which ablation is achieved by diphtheria toxin (DTX) administration, to describe new roles for DCs that are also independent of their immunological virtues (18–25). Using this mouse model, we recently showed that CD11c-positive cells are essential for successful embryo implantation via their effects on decidual tissue remodeling, independent of their immunologic anticipated role in the establishment of maternal-fetal tolerance (22). The loss of DCs using the DTR mouse model is especially attractive because the DTX causes cell death in nondividing, terminally differentiated cells and does so by inducing apoptosis. Because the toxin induces apoptosis by inhibition of protein synthesis and activating components of the death receptor pathway, there is no induction of inflammation after DTX administration (26, 27). Accordingly, studies that used the CD11c-DTR mouse model could not detect cell infiltration or inflammation in response to DTX-induced cell death. Because clearance of apoptotic cells does not induce a proinflammatory immune response, the depletion via DTX can be considered to occur under conditions of immunological steady state (21, 28).

The objective of the current study was to examine the ovaries for the presence of DCs, follow their possible accumulation in response to the ovulatory stimulus, unveil their function in ovulation and decipher their mechanism of action.

Materials and Methods

Animals

Sexually immature (24-day-old) transgenic CD11c-DTR$^{+/-}$ female mice (B6.FVB-TgItgax-DTR/green fluorescent protein [GFP] 57Lan/J) harboring a gene encoding a DTR/GFP fusion protein (23), transgenic CD11c-enhanced yellow fluorescent protein (EYFP), and wild-type C57BL/6 mice were purchased from Harlan Laboratories. Animals were handled at the Animal Breeding Center of the Weizmann Institute of Science according to the guidelines of the Weizmann Institute Animal Care and Use Committee.

Experimental protocols

Ovulation was induced by intraperitoneal administration of human chorionic gonadotropin (hCG) (5 IU; Organon) to pregnant mare serum gonadotropin (PMSG) (5 IU; Chronogest; Intervet)–primed female mice. At different time intervals (0, 4, 8, 12, 16, 20, and 24 hours) after hCG administration, mice were killed and their ovaries recovered.

Conditional depletion of CD11c-positive cells

For systemic depletion of DCs, female CD11c-DTR transgenic mice, expressing a primate DTR, were intraperitoneally injected with 2 to 4 ng of DTX (D-0564; Sigma-Aldrich) per gram of body weight, 24 hours after PMSG administration. For local DC depletion, DTX (0.1, 0.5, 1, 5, 10, and 20 ng) was injected into the ovarian bursa of CD11c-DTR transgenic female mice. As controls, CD11c-DTR and C57BL/6 mice were administrated either PBS or DTX, respectively.

Effect of DC depletion on cumulus expansion/mucification

Cumulus-oocyte complexes (COCs) recovered from either DTX-treated or untreated CD11c-DTR transgenic mice at 8 hours after hCG administration were analyzed. For that purpose, the mice were killed, and their ovaries were removed. The large antral follicles were punctured and the COCs were released and inspected under a dissecting microscope. The numbers of expanded and compact COCs and the number of denuded oocytes in each ovary was monitored.

airSEM imaging of COCs

COCs were recovered from either DTX-treated or untreated CD11c-DTR transgenic mice at 8 hours after hCG administration and imaged by *airSEM*. The *airSEM* (B-Nano Ltd.) is a novel imaging platform centered around a unique scanning electron microscope operating in open air (29). It operates in a direct correlative manner as follows: the sample is first imaged in the optical microscope for orientation and region of interest selection followed by its shuttled to the scanning electron microscope optical axes with accurate registration. Before imaging, recovered COCs were immersed in fixation solution containing polycationic dye, ruthenium red, followed by staining with uranyl acetate, a procedure that was recently developed for specific *airSEM* imaging of biological tissues (Solomonov, I., D. Talmi-Frank, Y. Milstein, S. Addadi, A. Aloshin, and I. Sagi, manuscript submitted for publication). Images were acquired by backscattered channel, the beam energy was 30 kV, and the probe current was 500 pA.

Allogeneic ovary transplantations

Ovaries from sexually immature 22-day-old C57BL/6 female mice were transplanted under the kidney capsule of EYFP-DC11c transgenic hosts, as described elsewhere (30). Six to 7 days later, host mice were treated with PMSG-hCG for induction of ovulation as described previously. Transplanted ovaries recovered 24 hours after hCG administration were processed for histology and fluorescence microscopy.

Allogeneic transplantation of DCs into the ovarian bursa of DTX-treated CD11c-DTR mice

For generation of DCs from murine bone marrow, we used the procedure described by Lutz et al (31) with minor modifications. In brief, bone marrow cells from tibias and femurs of 5- to 6-week-old C57BL/6 mice were cultured in RPMI 1640 medium supplemented with 10% heat-inactivated fetal calf serum (HyClone), 2 mM L-glutamine, 1% sodium pyruvate, 1% nonessential amino acids (Sigma-Aldrich), 5×10^{-5} M β-mercaptoethanol, combined antibiotics, and 200 U/mL granulocyte macrophage colony-stimulating factor (GM-CSF) (ProSpec). Concentrations were adjusted to reach 4×10^6 cells/mL, and 10 mL was seeded in 100-mm Petri dishes (Falcon 351029). On day 3, another 10 mL of medium containing 200 U/mL GM-CSF was added to the plates. On day 6, half of the culture supernatant was replaced with fresh medium containing 200 U/mL GM-CSF. On day 8, nonadherent cells were collected, adjusted to 15×10^6 cells/mL, resuspended in fresh medium containing 100 U/mL GM-CSF, and seeded in 100-mm tissue culture plates (Falcon 353003) for 24 hours. On day 9, nonadherent cells were harvested, washed, and resuspended in PBS to reach 9×10^6 cells/mL before injection. A total volume of 10 μL of either this cell suspension or PBS was injected into the ovarian bursa of DTX-treated CD11c-DTR transgenic mice, at 4 hours before hCG administration. Ovulation was evaluated by counting the number of oocytes found in the oviduct at 24 h after hCG administration.

Flow cytometry analysis

Ovaries were dissociated (gentelMACS Dissociator, MACS Miltenyi Biotec), stained, and subjected to fluorescence-activated cell sorting FACS analysis (FACSCalibur cytometer, using CellQuest software; BD Bioscience). The staining reagents used included the phycoerythrin-coupled anti-CD11c antibody, antigen-presenting cell–coupled anti-F4/80 antibody, and 7-aminoactinomycin D (7AAD); all were purchased from eBioscience. The Fluorescence Minus One method was used to set proper gating.

Quantitative real-time PCR

RNA was extracted and cDNA was prepared as we described previously (32). Primers were designed with Primer Express software (Applied Biosystems) and analyzed with the BLAT program for their specificity. The PCR primer pairs are described in Supplemental Table 1Supplemental Table 1. Relative quantification of the mRNA was performed by using the StepOne system v2.1 (Applied Biosystems). Quantitative real-time PCRs (10 μL) were performed with 2 μL of cDNA, 2.5 pmol of each primer, and 5 μL of Fast SYBR Green Master Mix (Applied Biosystems). As an internal control, β_2-microglobulin was amplified in parallel for each sample and used for normalization. Results are expressed relative to the calibrator sample using the $2^{-(\Delta\Delta C_T)}$ method. Data are presented as $2-^{(\Delta\Delta C_T)}$ values (mean $\pm$ SEM) normalized to the same calibrator sample to facilitate comparison of fold change (y-axis) with treatment. The amplification process was monitored through the fluorescence of SYBR Green.

Mass spectrometry protein analyses of the extracellular matrix of COCs

COCs were recovered from large antral follicles of either DTX-treated or untreated CD11c-DTR transgenic mice at 8 h after hCG administration, as described above. The protein levels of versican V1 isoform (VACN-V1) and TNFAIP6 were measured using mass spectrometry. For this purpose, recovered COCs were incubated in hyaluronidase (1 μg/mL in PBS) for 5 minutes at 37°C and centrifuged, and the supernatants were collected for analysis. Samples were mixed in 200 μL of 0.1 M Tris/HCl containing 4% SDS and 0.1 M dithiothreitol and incubated at 95°C for 3 minutes. Samples were then alkylated for 20 minutes in 0.05 M iodoacetamide in 8 M urea. An FASP protein digestion kit (Protein Discovery) was used for SDS removal as follows. Samples were mixed with urea, centrifuged through a YM-30 membrane, and then digested overnight at 37°C with trypsin (Promega) in 0.05 M NH_4HCO_3. The filtrate was collected on the next morning and acidified with 5% formic acid. The samples were then ready for the first dimension of the 2-dimensional liquid chromatography.

Digested protein was separated offline (first dimension) on an UltiMate 3000 Capillary/Nano LC System using a strong cation-exchange column (300 μm inside diameter $\times$ 15 cm, packed with Bio-SCX, 5 μm; LC Packings). A 60 minute gradient of 0.1% formic acid-5% acetonitrile (A) and 0.1% formic acid-5% acetonitrile containing 500 mM ammonium acetate (B) was used to elute the peptides. Samples were segregated into 5 regions: 0 to 12, 12 to 24, 24 to 36, 36 to 48, and 48 to 60 minutes. Such concatenation yielded 24 combined fractions for subsequent second-dimension reversed-phase liquid chromatography. Each combined fraction was separated on an in-house–made reversed-phase column (75 μm inside diameter $\times$ 15 cm, packed with ReproSil-Pur C18AQ, 0.3 μm; Dr. Maisch GmbH). Mobile phase A consisted of 95% Milli-Q water, 5% acetonitrile, 0.1% formic acid, and 0.005% trifluoroacetic acid. Mobile phase B consisted of 90% acetonitrile, 0.1% formic acid, and 0.005% trifluoroacetic acid. Samples were analyzed in an LTQ-Orbitrap XL instrument (Thermo Fisher Scientific) operated in the positive ion mode. The mass spectrometer was operated in the data-dependent mode. Survey mass spectrometry scans were acquired in the Orbitrap with the resolution set to a value of 60 000. Up to the 7 most intense ions per scan were fragmented and analyzed in the linear trap. Raw spectra were processed using MASCOT (Matrix Science) against a UniProt mouse database. Search parameters included the fixed modification of carboxyamidomethylation on Cys, and variable modifications including oxidation on Met and deamidation on Asn and Gln. The search parameters were as follows: maximum 2 missed cleavages, initial precursor ion mass tolerance of 10 ppm, and fragment ion mass tolerance of 0.6 Da. To validate the datasets generated by mass spectrometry, database search files generated by MASCOT were imported into Scaffold and further analyzed from within Scaffold, using the spectral quantitative value display option with the following filter settings: Min Protein 99%; Min # Peptides 2; and Min Peptide 95%. Each biological replicate was imported into Scaffold and combined, and the numbers of assigned peptides and spectra in each biological replicates were used for protein identification and quantification. The integrated PeptideProphet and ProteinProphet algorithms were used to control for false discovery rate and the probabilities were set to a minimum of 95% and 99%, respec-

tively. At least 2 unique matched peptides per protein were required for confident protein identification.

Histology and immunohistochemistry

Ovaries were recovered at various time intervals after ovulation induction (PMSG-hCG protocol, as described above) from sexually immature (24-day-old) transgenic CD11c-DTR$^{+/-}$ female mice (B6.FVB-TgItgax-DTR/GFP 57Lan/J), transgenic CD11c-EYFP mice, and/or wild-type C57BL/6 mice. Tissues were fixed in Carnoy solution, embedded in paraffin, sectioned (4-μm thickness), and stained by hematoxylin and eosin (Sigma-Aldrich) To mark blood vessels, paraffin sections were stained for vascular smooth muscle cells (using anti-mouse α-smooth muscle actin [SMA] antibodies, catalog no. A5691; Sigma-Aldrich), as described previously (33). To mark the endothelial cells of lymphatic vessels, paraffin sections were stained for lymphatic vessel endothelial receptor 1 (LYVE-1) (using anti-mouse LYVE-1 antibodies, catalog no. 103PA50AG; RDI). To monitor the dynamics of DC11c-positive cells in the ovaries, transgenic CD11c-EYFP mice at different time intervals (0, 4, 8, 12, 16, 20, and 24 hours) after hCG were administered BSA-Rox (10 mg/mL in PBS, 10 μL/g animal; as described previously [34]), and killed 1 minute later. Paraffin sections of their ovaries were stained with anti-GFP (primary antibody: goat polyclonal anti-GFP, biotin [catalog. no. ab6658; Abcam]; secondary antibody: Cy2-conjugated streptavidin, catalog no. 016–220-084; Jackson ImmunoResearch) and with Hoechst 33258 (Molecular Probes Invitrogen). Images were obtained either with an E800 microscope equipped with digital camera DXM 1200 (Nikon) or with a Pannoramic MIDI digital slide scanner (3DHISTECH). Imaging conditions were identical for all slides within each experiment.

Two-photon microscopy

Transgenic CD11c-EYFP mice were anesthetized by an intraperitoneal injection of ketamine (100 mg/kg, Ketaset; Fort Dodge Laboratories) and xylazine (10 mg/kg, XYL-M; VMD). Mice were intravenously injected with 2 fluorescent markers via a tail vain catheter. Specific nonselective staining of all the cell nuclei in the mouse was achieved by an injection of Hoechst 33258 (120 μL of 10 mg/mL). After 3 minutes, animals were administered Qtracker 655 nontargeted quantum dots (3 μL diluted in 150 μL of PBS; Invitrogen) to mark blood vessels. Two minutes later, the animals were killed by cervical dislocation, and the ovaries were removed for ex vivo imaging. Excised ovaries were placed in a carrier slide and imaged in an upright 2-photon microscope (Zeiss LSM 510 META NLO; equipped with a broadband Mai Tai HP femtosecond single-box tunable Ti-sapphire oscillator, with automated broadband wavelength tuning 700–1020 nm for 2-photon excitation [Spectra-physics]). Imaging was performed through $\times$10 and $\times$20 air lenses, 2-photon excitation with a wavelength of 920 nm, and emission at 650 to 700 nm (vessels), 535 to 590 nm (YFP), and 390 to 465 nm (nuclei). Images were processed using ImageJ software (National Institutes of Health).

Intravital microscopy of the ovary

CD11c-DTR$^{+/-}$ female mice were anesthetized by an intraperitoneal injection of ketamine and xylazine, as described above. To expose the ovary, a 10-mm incision was made in the skin and the dorsal abdominal wall ventrolateral to the lumbar area, just above the location of the ovary. The ovary was exposed by holding the adjacent fat pad with noncrushing forceps, and the ovarian bursa was removed. Mice were placed on a stage of a Zoom Stereo Microscope SZX-RFL-2 (Olympus) equipped with a fluorescence illuminator and a PixelFly QE charge-coupled device camera (PCO). The excitation and emission for the red filter set were 550 and 605 nm, respectively. Images were acquired using Camware camera-controlling software (PCO). For fluorescence visualization of the ovarian blood vessels, BSA-Rox (10 mg/mL in PBS, 10 μL/g animal, as described previously [34]) was injected using a tail vein catheter. Images were taken at 0, 1, 2, 3, 6, 9, 12, 15, 18, and 21 minutes after BSA-Rox administration, with a fluorescence exposure time of 10 ms. At the end of the imaging session, the animal was killed by cervical dislocation. Images were processed with ImageJ software. Regions of interest were selected as the entire ovary, and the mean signal intensity of the images at the different time points was normalized to the signal at $t = 1$ minute (representing the initial blood volume).

Progesterone assay

Serum progesterone concentrations were determined by the American Medical Laboratories (AML Israel Ltd), using a solid-phase, competitive chemiluminescence enzyme immunoassay (Immulite 2000 Progesterone Kit, catalog no. L2KPW2; Siemens Healthcare Diagnostics) performed on an Immulite 2000 Systems Analyzer. The lower progesterone detection limit was 0.2 ng/mL.

Statistical analyses

Comparisons between groups were performed with either ANOVA or Kruskal-Wallis nonparametric ANOVA using computer software (Statistix 8 Student Edition; Analytical Software). ANOVA was used to analyze normally distributed data (evaluated by the Shapiro-Wilk test) that had equal variances between groups (evaluated by a Bartlett test), whereas Kruskal-Wallis nonparametric ANOVA was used to analyze data that were not normally distributed and/or had unequal variance between groups. Pearson χ^2 test analysis was used to compare proportional data. Differences were considered significant at a value of $P < .05$. Data are presented as means $\pm$ SEM.

Results

DCs reside in the ovary and accumulate in the newly formed corpus luteum

To demonstrate the presence of ovarian DCs and to explore the possible change in their abundance in response to the ovulatory stimulus, ovaries recovered from sexually immature, PMSG-primed C57BL/6 female mice, before and at different time intervals after hCG administration, were subjected to FACS analysis (Figure 1, A–C). We observed that the abundance of CD11c-positive cells, present in the ovary even before treatment, gradually increased after hCG administration. These observations are consistent with previous reports of ovulation-associated

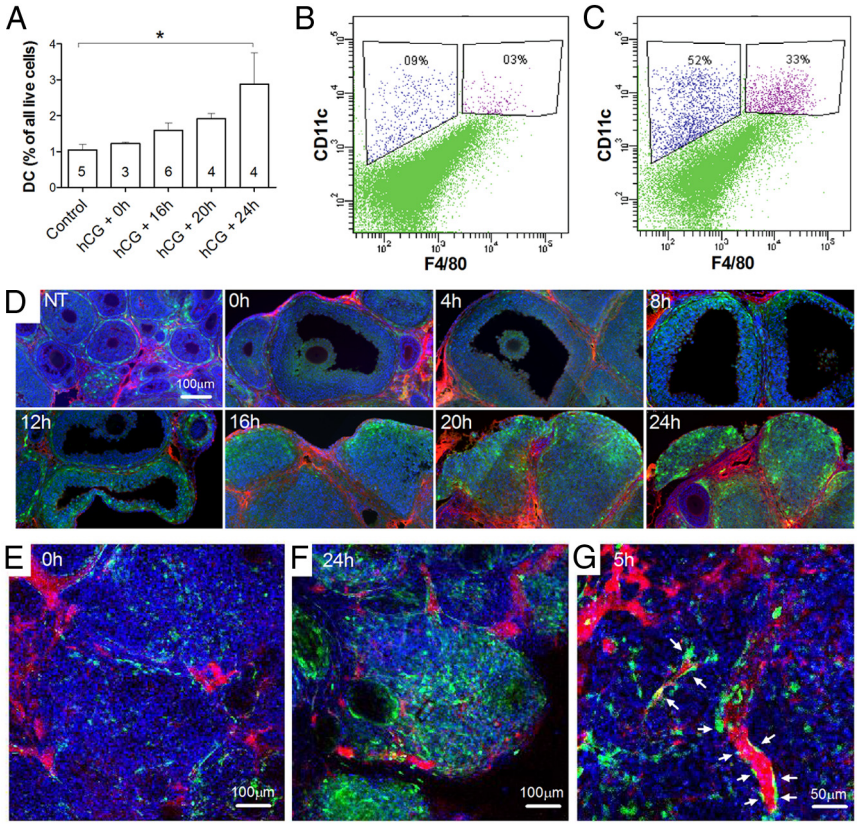

Figure 1. DCs reside in the ovary before ovulation and accumulate in the newly formed corpus luteum. A, FACS analysis of ovaries from sexually immature, PMSG-primed C57BL/6 female mice recovered before and at 16, 20, and 24 hours after hCG administration. Ovaries were dissociated into a single-cell suspension, stained with anti-CD11c fluorescent antibodies, and subjected to FACS analysis. Ovaries from nontreated mice (without hormones) served as controls. The number of repetitions, each consisting of 6 to 10 ovaries, is indicated at the bottom of the columns. Error bars represent SEM. *, $P < .05$. B and C, FACS analysis of ovaries recovered at 48 hours after PMSG administration (B) or at 24 hours after hCG administration to PMSG-primed C57BL/6 mice (C). Ovaries were dissociated, immunostained for CD11c, F4/80, and 7AAD, and subjected to FACS analysis. Only large 7AAD-negative (live) cells are presented. Proportions of gated cells of total large ovarian cells are indicated. n = 4 individual experiments, with 3 to 5 animals each. D, Fluorescence microscopy images of ovaries from CD11c-EYFP transgenic mice at different time intervals after hCG administration demonstrating the dynamic accumulation of CD11c-positive cells (green, CD11c-positive cells; red, blood vessels, BSA-Rox; blue, nuclei, Hoechst). NT, ovaries of nontreated sexually immature mice (without hormones). E, Ex vivo 2-photon microscopy image of ovaries recovered from CD11c-EYFP transgenic mice at 48 hours after PMSG administration, demonstrating a small number of CD11c-positive cells between and around preovulatory follicles (green, CD11c-positive cells; red, blood vessels, Qtracker 655 nontargeted quantum dots; blue, nuclei, Hoechst; scale bar corresponds to 100 μm). F, Ex vivo 2-photon microscopy image of ovaries recovered from PMSG-primed CD11c-EYFP transgenic mice at 24 hours after hCG administration demonstrating a large amount of CD11c-positive cells in a newly formed corpus luteum (green, CD11c-positive cells; red, blood vessels, Qtracker 655 nontargeted quantum dots; blue, nuclei, Hoechst; scale bar corresponds to 100 μm). G, Ex vivo 2-photon microscopy image of ovaries recovered from PMSG-primed CD11c-EYFP transgenic mice at 5 hours after hCG administration demonstrating CD11c-positive cells near and within the wall of blood vessels located in the ovarian interstitium (green, CD11c-positive cells; red, blood vessels, Qtracker 655 nontargeted quantum dots; blue, nuclei, Hoechst; scale bar corresponds to 50 μm).

massive ovarian infiltration by white blood cells (11). However, the major leukocyte population described so far is the F4/80-expressing macrophages (35), whereas our study revealed that in addition to the CD11c-positive, F4/80-positive cells (0.3% of large, live ovarian cells) (Figure 1B), F4/80-negative cells, apparently representing DCs, were also present at 48 hours after PMSG administration (0.9% of live ovarian cells) (Figure 1B) and significantly expanded at 12 hours after ovulation (5.2% of large live ovarian cells) (Figure 1C). Supporting these findings, histological fluorescence microscopy and ex vivo 2-photon microscopy examinations of ovaries of CD11c-EYFP mice (13) identified the typical dendritic morphology of these cells and demonstrated their dynamic accumulation as ovulation approaches (Figure 1, D–G and Supplemental Videos 1–3). A small number of these cells was detected between follicles before hCG hormonal stimulation (Figure 1, D and E and Supplemental Video 1), whereas after hCG administration, a large number of cells with dendritic morphology was observed within the follicular wall (theca layer) between the preovulatory follicles and later in the newly formed corpora lutea (Figure 1, D and F and Supplemental Videos 2 and 3). Many of the CD11c-positive cells were observed in close proximity and within the wall of blood vessels, suggesting that these cells may be recruited to the ovary from the circulation (5 hours after hCG administration) (Figure 1G and Supplemental Figure 1).

For a higher level of resolution, sorted ovarian CD11c-positive, F4/80-positive, and CD11b-negative cells were further analyzed for the 2 DC maturation markers major histocompatability complex class II (MHCII) and CD86, as well as for CD8α (36). FACS analysis performed at 12 hours after ovulation indicated that only 20.56% of the ovarian DCs express MHCII and only 13.2% express the CD86 molecule. In addition, the vast majority of ovarian DCs (95.2%) were characterized as CD8α-negative cells.

Allogeneic ovary transplantations were performed to further elucidate the recruitment of DCs into the ovary after hormonal stimulus. For that purpose, ovaries from sexually immature C57BL/6 female mice were trans-

planted under the kidney capsule of EYFP-CD11c transgenic hosts (30). Histological examinations revealed the formation of new blood vessels and the presence of follicles at various stages of development (Supplemental Figure 2A), indicating successful transplantation. Fluorescence microscopy detected CD11c-positive cells that migrated into the transplanted ovaries of these mice induced to ovulate by PMSG-hCG with accumulation particularly in the newly formed corpora lutea (Supplemental Figure 2B). Only a small population of DCs was identified around the follicles of the transplanted ovary in the absence of hormonal treatment. These results support the recruitment of DCs to the ovary from the circulation upon hormonal stimulation.

Conditional depletion of CD11c-positive cells blocked hCG-induced ovulation

To study the function of ovarian DCs in vivo, we used the previously established model of CD11c-DTR transgenic mice, the CD11c-positive cells of which express the simian DTR (18–25). PMSG-primed CD11c-DTR mice were treated with DTX 24 hours before hCG administration, thus, depleting the CD11c-positive cells before the onset of the ovulatory response (Figure 2A). FACS analysis confirmed that DTX treatment depleted the vast majority (93%) of CD11c-positive cells in the ovaries of CD11c-DTR mice (Supplemental Figure 3). Intraperitoneal DTX administration significantly reduced the number of ovulated oocytes of CD11c-DTR mice, with no such effect obtained upon either PBS injection to the transgenic animals or DTX administration to wild-type C57BL/6 mice (Figure 2B and Supplemental Figure 4A, respectively). This observation was complemented by histological examination that failed to detect ruptured follicles but identified, in ovaries of CD11c-ablated mice, oocytes trapped within corpora lutea (Figure 2D). Neither weight differences nor gross morphological abnor-

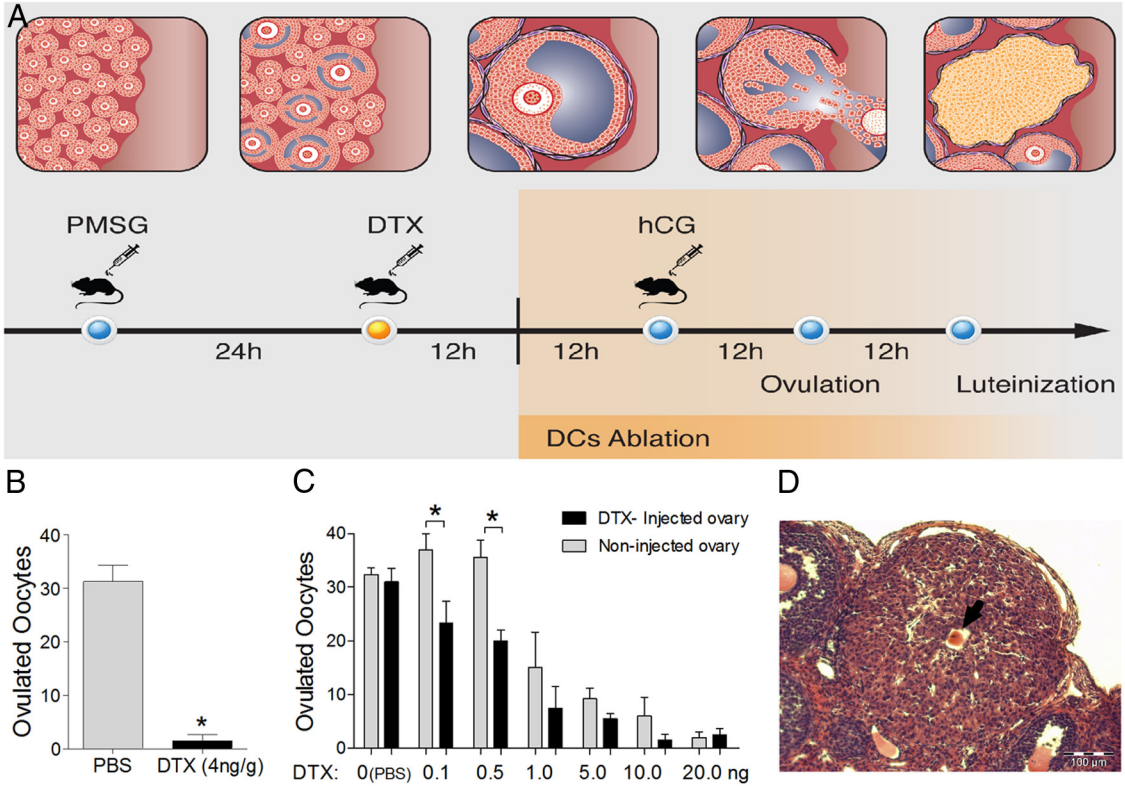

Figure 2. Conditional depletion of CD11c-positive cells blocks hCG-induced ovulation. A, Experimental model: conditional depletion of CD11c-positive cells. CD11c-DTR transgenic mice, in which expression of simian DTR is under the control of the DC promoter sequence CD11c, were used to study the function of DCs in vivo. PMSG-primed CD11c-DTR mice were treated with DTX 24 hours before hCG administration, thus depleting the CD11c-positive cells before the onset of the ovulatory response. B, Ovulated oocytes recovered from CD11c-positive cell–depleted mice compared with those from control mice. Sexually immature CD11c-DTR transgenic mice were treated with either DTX or PBS 24 hours before hCG administration. Ovulated oocytes were recovered from their oviducts 24 hours after hCG administration. Each column presents the mean number of ovulated oocytes per ovary (PBS, n = 16 mice; DTX, n = 22 mice). Error bars represent SEM. *, $P < .05$. C, Ovulated oocytes recovered after local depletion of CD11c-positive cells. DTX (0, 0.1, 0.5, 1, 5, 10, and 20 ng) was injected unilaterally into the ovarian bursa of sexually immature, PMSG-primed CD11c-DTR female mice at 24 hours before hCG administration (injected ovary), whereas the contralateral ovary remained untreated (noninjected ovary). Ovulated oocytes were recovered separately from each oviduct at 16 hours after hCG administration. The effect of DTX administration was dose dependent ($P < .05$). n = ≥6 mice/group; error bars represent SEM. D, Hematoxylin and eosin–stained histological section of an ovary of a CD11c-depleted mouse showing a trapped oocyte (indicated by black arrow) that resides within the corpus luteum (scale bar corresponds to 100 μm).

malities could be detected in the ovaries of the CD11c-ablated mice (Supplemental Figure 5).

To eliminate a possible effect of DTX directly on oocytes, isolated oocytes from wild-type C57BL/6 and from CD11c-DTR mice were incubated in DTX-containing medium. The oocytes resumed the meiotic division, progressing to the second metaphase as indicated by the presence of the first polar body (Supplemental Figure 4).

Unilateral injection of DTX into the ovarian bursa of CD11c-DTR mice, performed to rule out a general systemic effect, resulted, as expected, in failure of the respective ovary to ovulate. The effect of intrabursal DTX administration was dose dependent ($P < .05$) (Figure 2C). Furthermore, when DTX doses were low (≤5 ng), only the injected ovary was affected; however, a partial inhibition of ovulation also occurred in the nontreated contralateral ovary upon administration of a high dose of DTX (≥1 ng), possibly due to leakage to the circulation.

The effect of CD11c cell ablation after a single systemic injection of DTX was transient, with 70% of the CD11c-DTR mice responding to the commonly used protocol for stimulation of ovulation by PMSG-hCG administration, at 8 days after DTX treatment (n = 32 mice, $P < .05$).

Allogeneic transplantation of DCs into the ovarian bursa of DTX-treated CD11c-DTR mice restores ovulation

DCs were obtained from the bone marrow of wild-type C57BL/6 mice and purified as described under *Materials and Methods*. Only nonadherent cells were examined by flow cytometry; the purified population consisted of 92% to 97% CD11c-positive cells of which 88% to 96% were also CD11b-positive, 0.5 to 2.5% were F4/80-positive, and 0.02 to 0.2% were CD8α-expressing cells. Further characterization of these immature bone marrow–derived CD11c-positive cells revealed expression of low levels of both MHCII and costimulatory CD86 molecules. Injection of these cells directly into the ovarian bursa of PMSG-hCG-treated CD11c-DTR mice restored ovulation, evaluated by the number of oocytes found in the oviduct at 24 hours after hormonal stimulation (Figure 3A). The injection of these cells also restored the ovulation-associated expression levels of Adamts1 mRNA at 24 hours after hCG administration, which was downregulated upon DC ablation (Figure 3B).

Conditional depletion of CD11c-positive cells reduced the expression of ovulatory-essential genes, impaired cumulus cells mucification/expansion, and increased the expression of ovarian proinflammatory genes

To elucidate the mechanism by which DCs regulate ovulation, quantitative RT-PCR analysis was performed on ovaries recovered from PMSG-primed, DTX-treated CD11c-DTR mice at 4 hours after hCG administration (Figure 3C). Analyses showed no differences in the mRNA encoding for LH receptor (*Lhcgr*) in hGC-treated CD11c-ablated compared with hCG-treated CD11c-intact mice. Furthermore, at 4 hours after hCG treatment, the mRNA expressions of both epiregulin (*Ereg*) and amphiregulin (*Areg*) were similar in CD11c-ablated and in CD11c-intact mice, suggesting that the LH receptor was activated. However, analyses revealed that the ablation of CD11c cells impaired the hCG-induced expression of genes necessary for ovulation such as progesterone receptor (*Pgr*) and disintegrin metalloproteinase with thrombospondin-like repeats (*Adamts1*) (37, 38). Administration of hCG to CD11c-depleted mice also failed to up regulate genes that encode for *Tnfaip6*, and *Vcan-V1*. The latter genes are essential for stabilization of the extracellular matrix responsible for cumulus mucification/expansion, which is a prerequisite for ovulation (39, 40).

The effect of the CD11c-positive cell depletion on cumulus mucification/expansion was further evaluated by morphological examination of the COCs under a dissecting microscope (Figure 4A). As expected, a large fraction of the COCs underwent expansion after hCG administration. However, upon administration of hCG to DTX-treated mice, most of the oocytes recovered were denuded. Furthermore, even in the small fraction of COCs that display an expanded appearance, the cumulus cells were easily dissociated. To examine the hyaluronan-rich extracellular matrix in a higher resolution, COCs were recovered from either DTX-treated or untreated CD11c-DTR transgenic mice, at 8 hours after hCG administration, and imaged by *airSEM*. The *airSEM* imaging revealed abnormally low amounts of extracellular matrix between cumulus cells in CD11c-depleted mice (Figure 4, B to C). Mass spectrometry analysis showed lower protein abundance of TNFAIP6 and VCAN-V1 in the extracellular matrix of COCs that were recovered from CD11c-DTR transgenic, hCG-administered, DTX-treated mice than in mice that were not treated by the toxin (Figure 4D). These findings indicated a role for DCs in the stabilization of the extracellular matrix that holds together the cumulus cells of the expanded COC.

In addition to its role in the stabilization of the extracellular matrix, *Tnfaip6* is also a potent anti-inflammatory agent (41, 42). Another immune regulator, the elevated expression of which in response to hCG was observed in wild-type animals (Supplemental Figure 6) but not in CD11c-depleted mice (Figure 3C), is the pituitary adenylate cyclase–activating polypeptide (*Adcyap1*). In association with the low mRNA expression of these 2 genes encoding for the anti-inflammatory agents

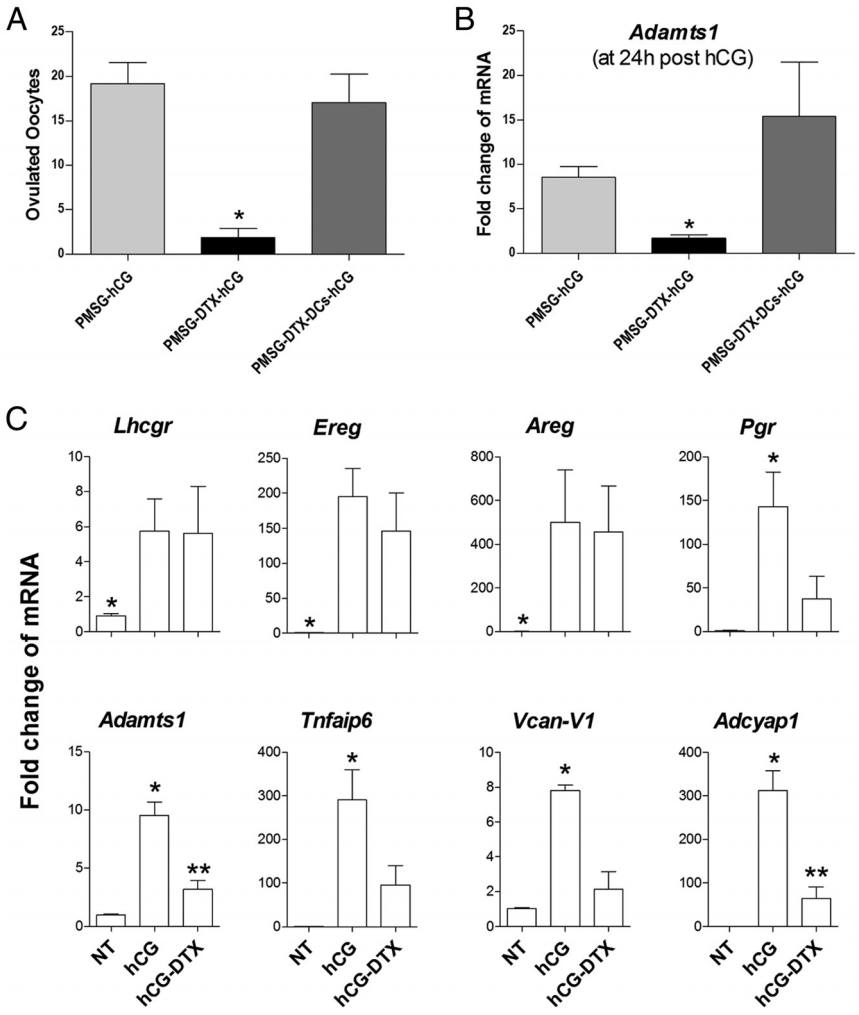

Figure 3. The presence of CD11c-positive DCs in the ovary is essential for ovulation and for the expression of hCG-induced ovulatory genes. A, Allogeneic transplantation of DCs into the ovarian bursa of hCG-stimulated, DTX-treated CD11c-DTR mice restores ovulation. The graph presents the number of oocytes ovulated after hormonal treatment (PMSG-hCG), hormonal treatment after depletion of CD11c-positive cells (PMSG-DTX-hCG), and the combination of hormonal treatment and DTX administration with allogeneic transplantation of DCs into the ovarian bursa (PMSG-DTX-DCs-hCG). Sexually immature CD11c-DTR transgenic mice were treated as described, and ovulated oocytes were recovered from their oviducts 24 hours after hCG administration. Each column presents the mean number of ovulated oocytes per oviduct. n = 15 mice. Error bars represent SEM. *, $P < .05$. B, Allogeneic transplantation of DCs into the ovarian bursa of hCG-stimulated, DTX-treated CD11c-DTR mice restored *Adamts1* mRNA expression. Graph presents quantitative real-time PCR analyses of *Adamts1* at 24 hours after hCG administration. Ovaries were recovered from CD11c-DTR transgenic mice after either hormonal treatment (PMSG-hCG), hormonal treatment after the depletion of CD11c-positive cells (PMSG-DTX-hCG), or the combination of hormonal treatment and DTX administration with allogeneic transplantation of DCs into the ovarian bursa (PMSG-DTX-DCs-hCG). n = 15 mice. Error bars represent SEM. *, $P < .05$. C, Quantitative real-time PCR analyses of genes essential for ovulation at 4 hours after hCG administration. Ovaries were recovered from DC-depleted (hCG-DTX), nondepleted (hCG), and untreated (NT) CD11c-DTR mice. n = ≥4 individual experiments, each including 4 mice/group. Error bars represent SEM. *, $P < .05$. Columns with different markings (* vs ** vs no marking) are significantly different.

in CD11c-depleted mice, we found in their ovaries a significant up-regulation of inflammation-associated genes, such as *Il1b*, *Tnf*, *Il6*, *Egr1*, *Ccl2*, and *Cxcl2* (Figure 5A). In contrast, expression of genes encoding for *Has2* and *Ptgs2* (43, 44) was unaffected. The mRNA expression of all these inflammation-associated genes was not altered when DTX was administered to wild-type C57BL/6 mice (Supplemental Figure 6).

Depletion of CD11c-positive cells altered blood vessel permeability and interfered with the development of ovarian lymphatic vessels

DCs were reported previously to be involved in the regulation of angiogenesis in various tissues (45). Accordingly, in the current study, immunohistochemical analysis of ovarian sections of mice administered hCG for the blood vessel marker α-SMA revealed a significant elevation of blood vascularity, particularly in the newly developed corpora lutea. Surprisingly, depletion of CD11c-positive cells by DTX did not appear to alter ovarian blood vessel development (Figure 5B). In agreement with this last observation, the hCG-induced mRNA expression of vascular endothelial growth factor A (*Vegfa*), known to enhance angiogenesis, was not altered in the ovaries of these mice (Figure 5D). To gain further insights regarding the permeability of blood vessels in the luteal follicles after depletion of CD11c-positive cells, we monitored, at 24 h after hCG administration, the in vivo dynamics of a fluorescently labeled high-molecular-weight agent (BSA-Rox) injected intravenously (46) (Supplemental Figure 7). No significant difference in blood density (ie, the ovarian fluorescent signal 1 minute after BSA-Rox administration) could be detected in the ovaries of CD11c-ablated mice compared with ovaries of CD11c-DTR mice treated with PMSG-hCG only. Nevertheless, over time, signal intensity dynamics in the imaged ovaries of the CD11c-depleted mice demonstrated higher incremental increase rates, indicating higher accumulation of the BSA-Rox (Figure 5E).

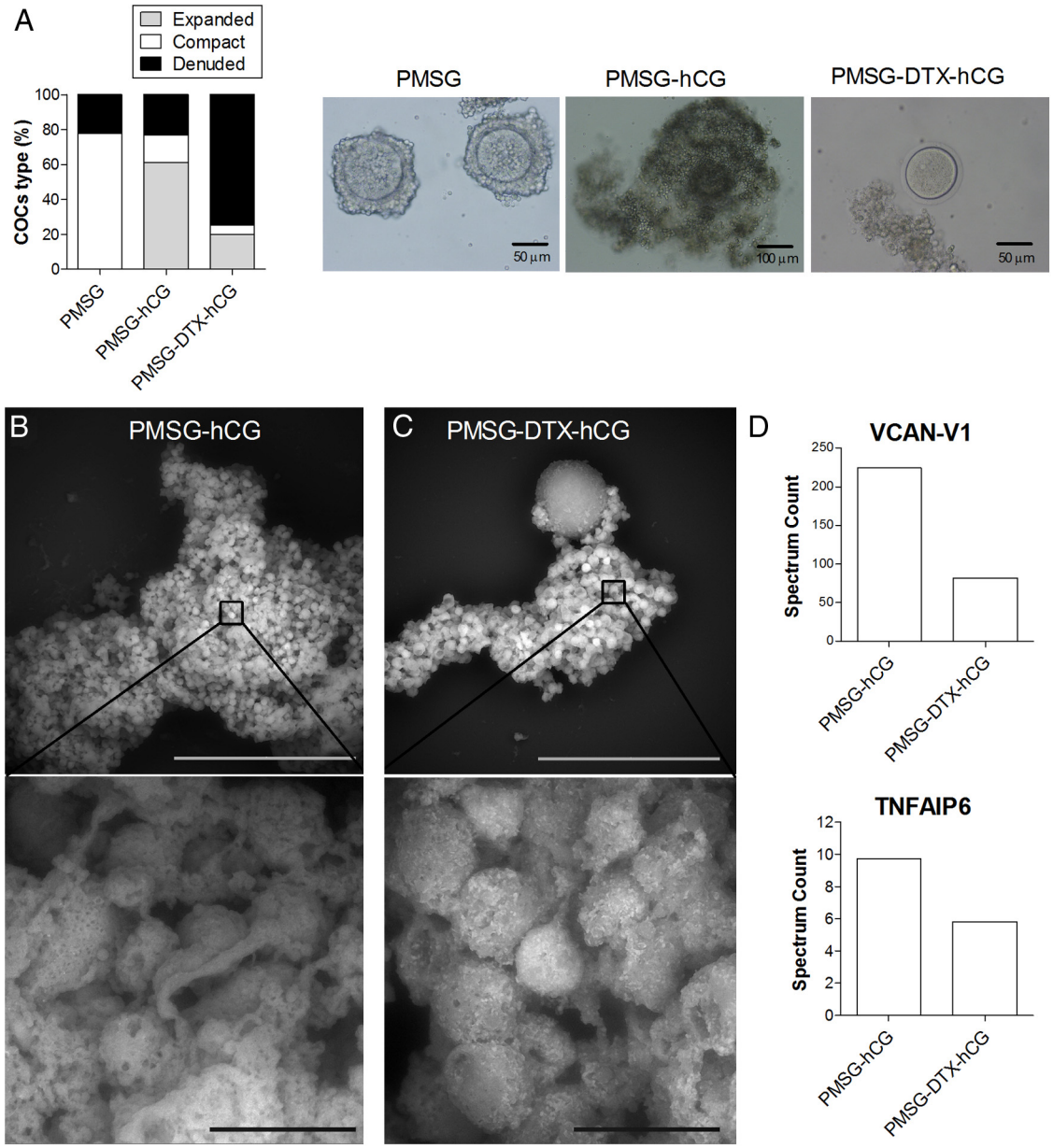

Figure 4. Cumulus cell mucification/expansion is depended on the present of CD11c-positive DCs in the ovary. A, Conditional depletion of CD11c-positive cells impaired cumulus cell mucification/expansion. The graph presents quantification of the morphological status of COCs (compact, expended, and denuded; shown in the right panels) as was evaluated by light microscopy. COCs were recovered from either ovaries of PMSG-primed mice with or without hCG administration (at 8 hours) or PMSG-primed mice treated by DTX followed by hCG administration. Most COCs in PMSG-primed mice were compact and expended after hCG administration; however, many of the COCs recovered from CD11c-depleted mice contained denuded oocytes (scale bar corresponds to 100 μm). B and C, Scanning electron microscopy (*airSEM*; backscattered with beam energy of 30 kV and probe current of 500 pA) of COCs recovered from PMSG-primed CD11c-DTR transgenic, either DTX-treated (C) or DTX-untreated (B), mice at 8 hours after hCG administration. Note the abnormal appearance and low amount of extracellular matrix between the cumulus cells of CD11c-depleted mice (scale bar corresponds to 100 μm (upper images) and 10 μm (bottom images). D, Mass spectrometry protein analysis of VCAN-V1 and TNFAIP6 in the extracellular matrix of COCs recovered from PMSG-primed CD11c-DTR transgenic, either DTX-treated or DTX-untreated, mice at 8 hours after hCG administration.

Immunostaining of the LYVE-1 revealed severe retardation in the development of the ovarian lymphatic vessels in newly formed corpora lutea in the absence of CD11c-positive cells (Figure 4C). In accordance, depletion of CD11c-positive cells by DTX treatment of CD11c-DTR mice abrogated the ability of hCG to induce the expression of *Adamts1* and *Vegfc* (Figures 3C and 5D, respectively), which are both prolymphangiogenic factors in the ovary (47, 48).

Depletion of CD11c-positive cells inhibited progesterone production

We speculated that the extensive alterations in the CD11c-depleted ovary might affect the steroidogenic ca-

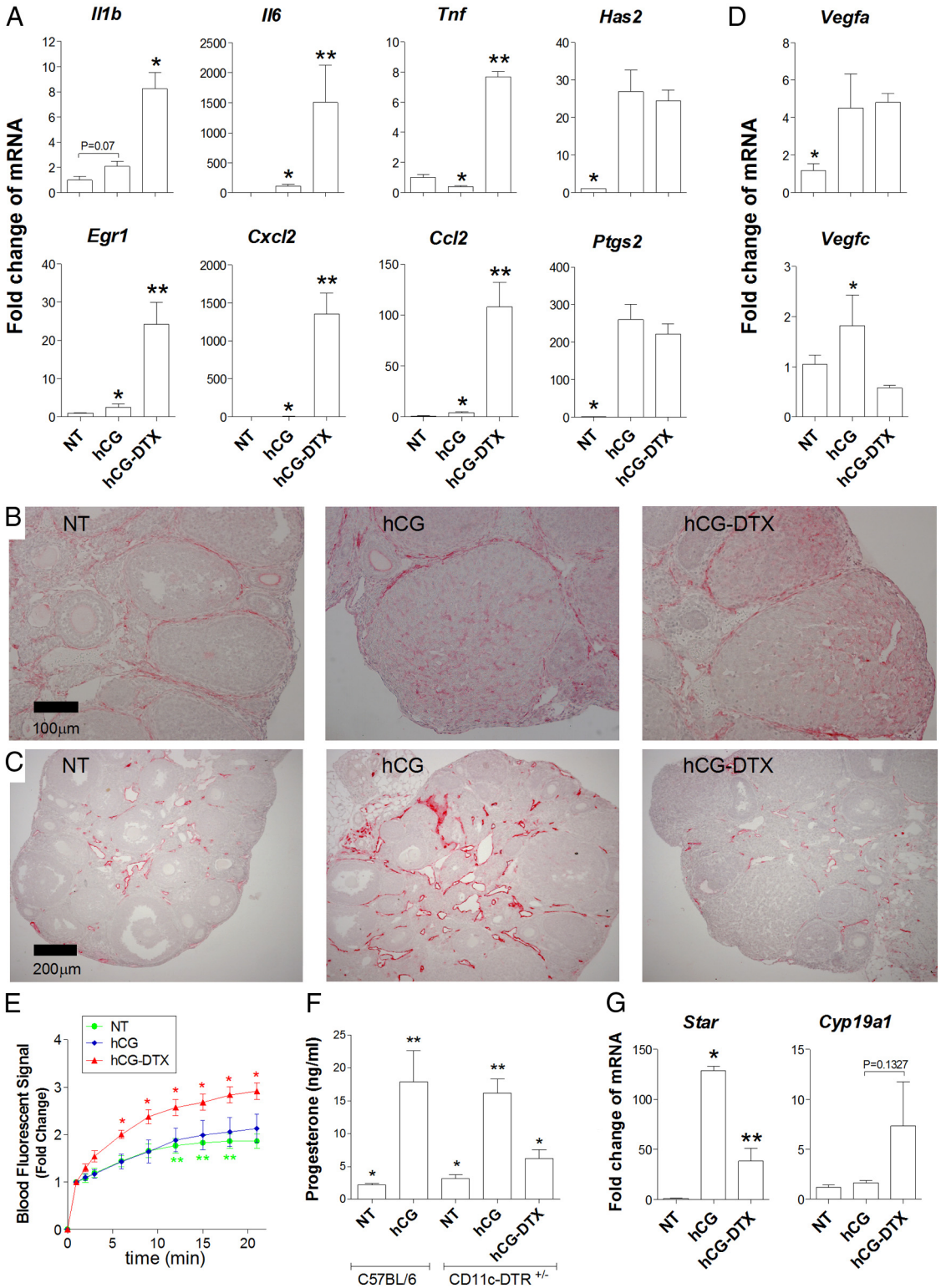

Figure 5. Depletion of CD11c-positive cells alters ovarian inflammatory gene expression, lymphatic vessel development, and progesterone production. A, Quantitative real-time PCR analyses of inflammation-associated genes. Ovaries were recovered at 4 hours after hCG administration from DC-depleted (hCG-DTX), nondepleted (hCG), and untreated (NT) CD11c-DTR mice. n = 4 individual experiments, each including 4 mice/group. Error bars represent SEM. *, $P < .05$. B, Immunostaining for the blood vessel marker α-SMA performed on ovaries recovered 20 hours after hCG administration from DC-depleted (hCG-DTX), nondepleted (hCG), and untreated (NT) CD11c-DTR mice, demonstrating an hCG-stimulated increase in ovarian blood vessels, particularly in the newly developed corpora lutea, that was not altered by depletion of CD11c-positive cells (n = 5 mice, 10 ovaries/group; scale bar corresponds to 100 μm). C, Immunostaining for LYVE-1 shows a significant increase in the ovarian lymphatic vessels after hCG administration that was severely impaired by the depletion of CD11c-positive cells (n = 5 mice, 10 ovaries/group; scale bar corresponds to 200 μm). D, Quantitative real-time PCR analyses of *Vegfa*, and *Vegfc*. Ovaries were recovered at 4 hours after hCG

pacity of the corpus luteum. Indeed, in animals depleted of CD11c-positive cells, we determined a substantially lower concentration of serum progesterone, the major steroid hormone produced by the corpus luteum (Figure 5F). In agreement with this finding, a low expression of the mRNA encoding for steroidogenic acute regulatory protein (STAR), a key protein for steroidogenesis, was found in ovaries of hCG-treated, CD11c-depleted mice at 4 hours after hCG administration (Figure 5G). Furthermore, at this time point, the mRNA expression of the gene that encodes for P450 aromatase, *Cyp19a1*, tended ($P = .1327$) to be higher in the ovaries of the DTX-treated, CD11c-DTR transgenic mice compared with these same mice that were not treated by the toxin (Figure 5G). It was previously shown that down-regulation of *Cyp19a1* after LH stimulation is essential for luteinization, during which the estradiol-producing granulosa cells are transformed to progesterone-producing luteal cells (44, 49, 50).

Discussion

We show herein that CD11c-positive, F4/80-negative cells, apparently representing DCs, reside in the ovary before ovulation. In response to the ovulatory stimulus provided by hCG, these cells gradually accumulate in the preovulatory follicles and overpopulate the newly formed corpus luteum. Our study further provides evidence for the crucial role of these cells in ovulation. Specifically, we demonstrated that after the depletion of these cells ovulation failed. These findings are strongly complemented by allogeneic transplantation of DCs into the ovarian bursa of CD11c-depleted mice that restored ovulation. Further mechanistic experiments provide evidence that these cells take part in the hCG-induced up-regulation of ovulation-essential genes, with no effect on the expression of the LH receptor or its activation (ie, no changes in the expression of *Areg* and *Ereg*). We also show that not only follicle rupture but also the formation of a functional corpus luteum is fully dependent on these DCs. Unexpectedly, our data also suggest that these cells mediate the expression of a set of anti-inflammatory genes, apparently involved in the restraint of the physiologic ovulatory-associated inflammation (1, 2).

Previous studies showed that under gonadotropin regulation there is a massive infiltration of a white blood cell subset to the ovary (11, 51–53). Our study detected in the ovary a specific population of leukocytes displaying dendritic morphology, which express CD11c but not F4/80, apparently representing DCs. This finding is in agreement with a recent study that identified CD11c-positive cells in the follicular fluid aspirated from the ovaries of women undergoing fertility treatments in an in vitro fertilization clinic (54). To study the function of these cells in vivo we employed the strategy of conditional ablation of CD11c-positive cells using the CD11c-DTR transgenic mouse model (18–25). DTX was administered to these mice, either systemically or to the ovarian bursa 24 hours before hCG with the aim of depleting the DCs before the onset of the ovulatory response.

CD11c is a type I transmembrane protein highly expressed by DCs (20, 23). However, a low level of expression of this protein was also reported for some subsets of macrophages, natural killer cells, and neutrophils (21). Accordingly, it has been shown previously that in addition to the desired specific depletion of CD11c-positive DCs, the administration of DTX to CD11c-DTR transgenic mice results in the ablation of marginal zone macrophages in the spleen and of sinusoidal macrophages in the lymph nodes (20, 21). Therefore, it cannot be ruled out that at least some of our findings obtained by the use of this transgenic mouse model are not solely the consequence of the massive ablation of DCs but also represent the depletion of other cell types. Taking into consideration previous reports of the high abundance of macrophages in the ovary (10, 52, 55), their contribution should be taken into account. However, our analysis revealed that the vast majority of macrophages (F4/80-positive, CD11b-positive cells) in the ovary at 24 hours after hCG administration do not express the CD11c marker (only 4.8% of ovarian macrophages are CD11b-, CD11c-, and F4/80-positive cells). Furthermore, conditional ablation of macrophages in a CD11b-DTR mouse, in which ex-

Figure 5. (Continued). administration from DC-depleted (hCG-DTX), nondepleted (hCG), and untreated (NT) CD11c-DTR mice. n = 4 individual experiments, each including 4 mice/group. Error bars represent SEM. *, $P < .05$. E, In vivo ovarian fluorescent signal dynamics of BSA-Rox injected intravenously at 24 hours after hCG administration to DC-depleted (hCG-DTX), nondepleted (hCG), and untreated (NT) PMSG-primed CD11c-DTR mice (n = 5 mice/group). For each animal, the ovarian fluorescent signal in each time point was normalized to the initial signal (ie, at 1 minute, associated with blood vessel density). Over time, the signal intensity dynamics in the imaged ovaries of the CD11c-depleted mice demonstrated higher incremental increased rate, indicating higher accumulation of the BSA-Rox in their ovaries. F, Serum progesterone concentrations of either CD11c-DTR (DTR) or wild-type (C57BL/6) mice. Serum progesterone concentrations were evaluated in untreated mice (NT) at 24 hours after hCG administration to either PMSG-primed nondepleted (hCG) or PMSG-primed, CD11c-depleted mice (hCG-DTX). n = 5 mice/group; error bars represent SEM. *, $P < .05$. G, Quantitative real-time PCR analyses of *Star* and *Cyp19a1*. Ovaries were recovered at 4 hours after hCG administration from DC-depleted (hCG-DTX), nondepleted (hCG), and untreated (NT) CD11c-DTR mice. n = 4 individual experiments, each including 4 mice/group. Error bars represent SEM. *, $P < .05$. Columns with different markings (* vs ** vs no marking) are significantly different.

pression of human DTR is under the control of the macrophage-specific promoter sequence CD11b, resulted in ovarian hemorrhage associated with a significant endothelial cell depletion and elevated erythrocyte accumulation, suggesting that macrophages play a critical role in maintaining ovarian blood vessel integrity (56). This phenotype is different from the one reported here for depletion of CD11c-positive cells. Furthermore, unlike the absence of an effect on progesterone production reported in a previous study that used intrabursal injections of clodronate liposomes for specific depletion of macrophages (57), we did find a significant reduction in serum progesterone after the depletion of CD11c-positive cells, as well as uncharacteristic expressions of *Star* and *Cyp19a1,* which are related to luteinization after hCG stimulation. Chun et al (58) reported that neutrophil depletion by vinblastine sulfate or cyclophosphamide administration neither prevented ovulation nor altered the rate of follicular rupture. In another study, Brännström et al (59) reported only a minor decrease in ovulation rate and no effect on progesterone production in rats treated with neutrophil-specific, cytotoxic RP-3 monoclonal antibody. Furthermore, natural killer cells, as well as T and B lymphocytes, have been shown to be unaffected in CD11c-DTR genetic mice after DTX injection (20, 23, 60).

Taken together, the different phenotypes obtained upon both macrophage and neutrophil depletion and our rescue results after allogeneic transplantation of DCs into the ovarian bursa strongly suggest that the findings reported in the current study upon the ablation of CD11c-positive cells are mostly attributed to the absence of DCs rather than that of the other immune cells.

The depletion of CD11c-positive cells in our study resulted in a severe reduction in the number of oocytes ovulated after gonadotropin stimulation. Histological analysis confirmed that after the depletion of CD11c-positive cells, follicle rupture was impaired, and oocytes remained trapped within the luteinizing follicles. These effects of DC ablation were associated with reduced expression of genes essential for ovulation. Specifically, in CD11c-depleted female mice, hCG failed to up-regulate the expression of the gene encoding for the progesterone receptor (*Pgr*). Previous studies have shown that null mutation of the *Pgr* gene (37, 61) or treatment with progesterone receptor antagonists (62–64) lead to failure of gonadotrophin to stimulate ovulation, resulting in oocytes trapped within unruptured follicles. Furthermore, *Adamts1*, another ovulation-associated gene, the expression of which in the ovary is stimulated by LH via the progesterone receptor (65, 66), also failed to rise in CD11c-depleted mice, in response to hCG administration. These findings are consistent with the demonstration of mature oocytes trapped in ovarian follicles in the *Adamts1*-null mice (67).

Analysis of the response of the COCs to the ovulatory stimulus revealed that the hCG-induced formation of the extracellular matrix (responsible for cumulus mucification/expansion) was severely affected by the depletion of CD11c-positive cells and that most of the oocytes were partially or fully denuded. Furthermore, our *airSEM* analyses clearly demonstrated a low amount and an abnormal appearance of the extracellular matrix between cumulus cells of CD11c-depleted mice. In accordance, administration of hCG to CD11c-depleted mice failed to up-regulate the mRNA and protein levels of *Vcan-V1* and of *Tnfaip6*, which are both essential for the stabilization of the extracellular matrix responsible for cumulus mucification/expansion (39, 68, 69). *Vcan-V1* is a preferred substrate of the protease *Adamts1*; both proteins are coordinately induced by the *Pgr*-mediated LH action and colocalize in cumulus cells of ovulating follicles (70). Considering this information, our data support the notion that ovarian DCs elicit a positive ovulatory response through their effect on cumulus mucification/expansion, a prerequisite for ovulation.

In an in vitro study, human DCs were found to produce high levels of *Tnfaip6* in response to proinflammatory mediators (lipopolysaccharides or cytokines) (42). In the ovary, the expression of *Tnfaip6* mRNA has been shown to be induced rapidly in granulosa/cumulus cells of preovulatory follicles (43, 68) and by an ovulatory dose of hCG, in association with expression of *Ptgs2* in the same cells (71). Interestingly, in the current study, the hCG-induced expression of *Ptgs2* was not affected upon depletion of CD11c-positive cells, suggesting that the expression of *Tnfaip6* and that of *Ptgs2* are subjected to different regulatory pathways.

Interestingly, along with the failure of hCG to stimulate the expression of the genes encoding for the 2 anti-inflammatory agents, *Tnfaip6* and *Adcyap1* (41, 72, 73), in ovaries of CD11c-depleted mice, we found in these ovaries a significant excess of the inflammation-associated genes. Therefore, we infer that CD11c-positive cells are involved in controlling the extent of the ovulatory-associated inflammatory response provoked by ovulation (1, 2). Indeed, participation of DCs in the reduction of inflammation has previously been shown after viral infection or allergen inhalation (14) and in the burden of commensal microbial stimuli in the intestine; however, our findings may indicate that these cells act in attenuating inflammation as part of a physiological event (ie, ovulation) unrelated to interaction with foreign antigens. Hence, our study discovers wide diversity and extended

capabilities of DCs, beyond their classic immunologic role, which are most likely relevant to many biological systems and pathological conditions. Considering the large repertoire of functions that can be attributed to DCs, it is theoretically possible that in addition to their role in ovulation, these immune cells may be involved in the pathophysiology of ovarian inflammatory-related diseases such as human ovarian hyperstimulation syndrome and polycystic ovary disease (74). Furthermore, other pathological conditions such as ovarian endometrioma and metabolic syndrome/obesity (10, 75), which involve ovarian dysfunction that may lead to infertility, as well as autoimmune diseases and consequently premature ovarian failure, may potentially involve these immune cells. Because DCs were not studied in the ovary until recently, additional research should be conducted to elucidate their direct interaction with the granulosa, theca, and cumulus cells for further evaluation of their possible involvement in these pathological conditions.

DCs were reported previously to facilitate angiogenesis in various tissues (45, 76–78). Furthermore, density and permeability of blood vessels have been shown to be affected under inflammatory conditions (79). In the current study, immunohistochemical analysis of ovarian sections for the blood vessel marker α-SMA and in vivo analyses of injectable BAS-Rox dynamics in the ovaries after ovulation could not detect changes in blood vessel density upon the depletion of CD11c-positive cells. However, our results may suggest that the permeability of the ovarian blood vessels in these animals was significantly increased. This can be attributed to the resultant severe ovarian inflammation, as was demonstrated by up-regulation of the proinflammatory gene and reduced expression of anti-inflammatory genes in CD11c-depleted ovaries. In addition, other parameters, such as blood flow, the number of capillaries perfused, and the capillary hydrostatic pressure, possibly could have been altered upon the depletion of CD11c-positive cells.

Lymphatic vessels are necessary for the maintenance of fluid homeostasis, protein balance and immune cell trafficking within tissues (80, 81). In the ovary, lymphangiogenesis is hormonally regulated during folliculogenesis and through the formation of a functional corpus luteum (82). We found severe retardation in the development of ovarian lymphatic vessels in the absence of CD11c-positive cells. This finding is in agreement with a recent report, which demonstrated that DC depletion markedly inhibited the lymphangiogenesis induced by T cells in tertiary lymphoid structures (19). We also found that in the ovaries of CD11c-depleted mice, hCG failed to stimulate the expression of the genes *Vegfc* and *Adamts1,* both of which are known to be positively associated with the development of lymphatic vessels (48, 47). We therefore suggest that DCs are essential for the LH-stimulated development of lymphatic vessels in the ovary; however, because the current report focused on the involvement of DCs in the ovulatory process, further studies are needed to investigate the mechanistic role of DCs in ovarian lymphangiogenesis.

In the current study, hCG failed to induce the proper production of progesterone in the absence of CD11c-positive cells. The extensive alterations in the inflammatory environment, vascular permeability, and lymphatic vessels during the lu-

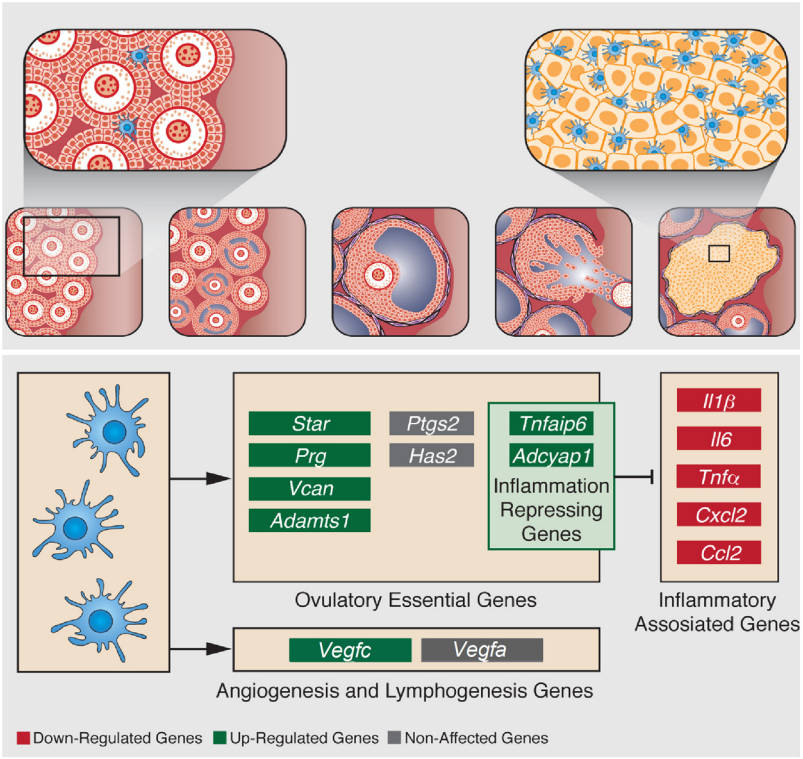

Figure 6. Model depicting the role of DCs in the ovary during ovulation. Upon gonadotropin stimulation, the relatively small ovarian DC population is essential for the LH-stimulated up-regulation of specific ovulatory genes that are crucial for cumulus mucification/expansion and ovulation. As the ovulatory process progresses, the ovarian DC population expands and localizes to the newly formed corpus luteum. During this process, up-regulation of the inflammatory repressing genes confine the inflammatory conditions provoked by ovulation. In the early luteal phase, the substantial amount of DCs localized in the newly formed corpus luteum facilitates progesterone production as well as ovarian lymphangiogenesis.

teinizing stage of the CD11c-depleted ovary may have impaired the steroidogenic capacity of the corpus luteum. However, this could represent direct involvement of DCs in regulation of ovarian steroidogenesis during ovulation. In concurrence with that hypothesis, we found that depletion of CD11c-positive cells significantly interfered with the stimulatory effect of hCG on the expression of the mRNA encoding for STAR, which is considered the rate-limiting factor in the production of steroid hormones (84). Furthermore, the mRNA expression of *Cyp19a1* at 4 hours after hCG stimulation was atypical; rapid reduction of *Cyp19a1* expression after LH stimulation is part of luteinization; however, in the current study it tended to be higher in the ovaries of the PMSG-hCG–administered, DTX-treated CD11c-DTR transgenic mice than in the mice that were not treated by the toxin. Additional studies should be conducted to further explore the possible effect of DC depletion on the steroidogenic capacities of granulosa and theca cells, as well as luteinizing cells, both in in vitro conditions and by depletion of CD11c cells after corpus luteum formation.

Based on observations presented herein, along with previously reported studies, we put forward the model for the role of DCs in ovulation shown in Figure 6. Upon gonadotropin stimulation, the relatively small ovarian DC population mediates the LH-stimulated up-regulation of specific genes, such as *Tnfaip6*, *Vcan-V1*, *Star*, *Pgr*, and *Adamts1* that are essential for cumulus mucification/expansion and ovulation. As the ovulatory process progresses, the ovarian DC population expands and localizes to the corpus luteum to control the inflammatory conditions provoked by ovulation. This activity is executed by suppressing proinflammatory factors such as *Il6*, *Il1*, *Tnf*, *Ccl2, Egr1*, and *Cxcl2*, which is secondary to up-regulation of the inflammatory repressing genes *Adcyap1* and *Tnfaip6*. In the early luteal phase, the substantial amount of DCs localized in the newly formed corpus luteum facilitates progesterone production as well as ovarian lymphangiogenesis.

Acknowledgments

We thank Prof Steffen Jung and Prof Alex Tsafriri from the Weizmann Institute for their comments, Tevi Mehlman from the Weizmann Institute for his assistance with the mass spectrometry analysis, and Yonat Milstein for help in the *airSEM* imaging.

Address all correspondence and requests for reprints to: Prof. Nava Dekel, Department of Biological Regulation, Weizmann Institute of Science, PO Box 26, Rehovot 76100, Israel. E-mail: nava.dekel@weizmann.ac.il.

This work was supported by the Dwek Fund for Biomedical Research (to N.D.), the Seventh Framework European Research Council (Advanced Grant 232640-IMAGO, and the Israel Science Foundation (93/07 [to M.N.] and 725/13 [to N.D.]).

Disclosure Summary: The authors have nothing to disclose.

References

1. **Espey LL.** Ovulation as an inflammatory reaction—a hypothesis. *Biol Reprod*. 1980;22:73–106.
2. **Richards JS, Liu Z, Shimada M.** Immune-like mechanisms in ovulation. *Trends Endocrinol Metab*. 2008;19:191–196.
3. **Tsafriri A, Lindner HR, Zor U, Lamprecht SA.** Physiological role of prostaglandins in the induction of ovulation. *Prostaglandins*. 1972; 2:1–10.
4. **Reich R, Kohen F, Slager R, Tsafriri A.** Ovarian lipoxygenase activity and its regulation by gonadotropin in the rat. *Prostaglandins*. 1985;30:581–590.
5. **Reich R, Daphna-Iken D, Chun SY, et al.** Preovulatory changes in ovarian expression of collagenases and tissue metalloproteinase inhibitor messenger ribonucleic acid: role of eicosanoids. *Endocrinology*. 1991;129:1869–1875.
6. **Chun SY, Popliker M, Reich R, Tsafriri A.** Localization of preovulatory expression of plasminogen activator inhibitor type-1 and tissue inhibitor of metalloproteinase type-1 mRNAs in the rat ovary. *Biol Reprod*. 1992;47:245–253.
7. **Abisogun AO, Braquet P, Tsafriri A.** The involvement of platelet activating factor in ovulation. *Science*. 1989;243:381–383.
8. **Kennedy CR, Zhang Y, Brandon S, et al.** Salt-sensitive hypertension and reduced fertility in mice lacking the prostaglandin EP_2 receptor. *Nat Med*. 1999;5:217–220.
9. **Parr EL.** Histological examination of the rat ovarian follicle wall prior to ovulation. *Biol Reprod*. 1974;11:483–503.
10. **Brännström M, Giesecke L, Moore IC, van den Heuvel CJ, Robertson SA.** Leukocyte subpopulations in the rat corpus luteum during pregnancy and pseudopregnancy. *Biol Reprod*. 1994;50:1161–1167.
11. **Suzuki T, Sasano H, Takaya R, et al.** Leukocytes in normal-cycling human ovaries: immunohistochemical distribution and characterization. *Hum Reprod*. 1998;13:2186–2191.
12. **Zhou C, Wu J, Borillo J, Torres L, McMahon J, Lou YH.** Potential roles of a special $CD8\alpha\alpha^+$ cell population and CC chemokine thymus-expressed chemokine in ovulation related inflammation. *J Immunol*. 2009;182:596–603.
13. **Lindquist RL, Shakhar G, Dudziak D, et al.** Visualizing dendritic cell networks in vivo. *Nat Immunol*. 2004;5:1243–1250.
14. **Lambrecht BN, Hammad H.** The role of dendritic and epithelial cells as master regulators of allergic airway inflammation. *Lancet*. 2010;376:835–843.
15. **Geissmann F, Manz MG, Jung S, Sieweke MH, Merad M, Ley K.** Development of monocytes, macrophages, and dendritic cells. *Science*. 2010;327:656–661.
16. **Steinman RM.** Avoiding horror autotoxicus: the importance of dendritic cells in peripheral T cell tolerance. *Proc Natl Acad Sci USA*. 2002;99:351–358.
17. **Guerin LR, Prins JR, Robertson SA.** Regulatory T-cells and immune tolerance in pregnancy: a new target for infertility treatment? *Hum Reprod Update*. 2009;15:517–535.
18. **Sapoznikov A, Jung S.** Probing in vivo dendritic cell functions by conditional cell ablation. *Immunol Cell Biol*. 2008;86:409–415.
19. **Muniz LR, Pacer ME, Lira SA, Furtado GC.** A critical role for dendritic cells in the formation of lymphatic vessels within tertiary lymphoid structures. *J Immunol*. 2011;187:828–834.
20. **Probst HC, Tschannen K, Odermatt B, Schwendener R, Zinkernagel RM, Van Den Broek M.** Histological analysis of CD11c-DTR/

GFP mice after in vivo depletion of dendritic cells. *Clin Exp Immunol*. 2005;141:398–404.
21. **Bennett CL, Clausen BE.** DC ablation in mice: promises, pitfalls, and challenges. *Trends Immunol*. 2007;28:525–531.
22. **Plaks V, Birnberg T, Berkutzki T, et al.** Uterine DCs are crucial for decidua formation during embryo implantation in mice. *J Clin Invest*. 2008;118:3954–3965.
23. **Jung S, Unutmaz D, Wong P, et al.** In vivo depletion of $CD11c^+$ dendritic cells abrogates priming of $CD8^+$ T cells by exogenous cell-associated antigens. *Immunity*. 2002;17:211–220.
24. **Bedrosian AS, Nguyen AH, Hackman M, et al.** Dendritic cells promote pancreatic viability in mice with acute pancreatitis. *Gastroenterology*. 2011;141:1915–1926.e1–14.
25. **Bar-On L, Jung S.** Defining in vivo dendritic cell functions using CD11c-DTR transgenic mice. *Methods Mol Biol*. 2010;595:429–442.
26. **Morimoto H, Bonavida B.** Diphtheria toxin- and Pseudomonas A toxin-mediated apoptosis. ADP ribosylation of elongation factor-2 is required for DNA fragmentation and cell lysis and synergy with tumor necrosis factor-α. *J Immunol*. 1992;149:2089–2094.
27. **Thorburn J, Frankel AE, Thorburn A.** Apoptosis by leukemia cell-targeted diphtheria toxin occurs via receptor-independent activation of Fas-associated death domain protein. *Clin Cancer Res*. 2003;9:861–865.
28. **Bennett CL, van Rijn E, Jung S, et al.** Inducible ablation of mouse Langerhans cells diminishes but fails to abrogate contact hypersensitivity. *J Cell Biol*. 2005;169:569–576.
29. **Vidavsky N, Addadi S, Mahamid J, et al.** Initial stages of calcium uptake and mineral deposition in sea urchin embryos. *Proc Natl Acad Sci USA*. 2014;111:39–44.
30. **Torrents E, Boiso I, Barri PN, Veiga A.** Applications of ovarian tissue transplantation in experimental biology and medicine. *Hum Reprod Update*. 2003;9:471–481.
31. **Lutz MB, Kukutsch N, Ogilvie AL, et al.** An advanced culture method for generating large quantities of highly pure dendritic cells from mouse bone marrow. *J Immunol methods*. 1999;223:77–92.
32. **Reizel Y, Elbaz J, Dekel N.** Sustained activity of the EGF receptor is an absolute requisite for LH-induced oocyte maturation and cumulus expansion. *Mol Endocrinol*. 2010;24:402–411.
33. **Plaks V, Kalchenko V, Dekel N, Neeman M.** MRI analysis of angiogenesis during mouse embryo implantation. *Magn Reson Med*. 2006;55:1013–1022.
34. **Dafni H, Landsman L, Schechter B, Kohen F, Neeman M.** MRI and fluorescence microscopy of the acute vascular response to VEGF165: vasodilation, hyper-permeability and lymphatic uptake, followed by rapid inactivation of the growth factor. *NMR Biomed*. 2002;15:120–131.
35. **Adashi EY.** The potential relevance of cytokines to ovarian physiology. *J Steroid Biochem Mol Biol*. 1992;43:439–444.
36. **Naik SH, Sathe P, Park HY, et al.** Development of plasmacytoid and conventional dendritic cell subtypes from single precursor cells derived in vitro and in vivo. *Nat Immunol*. 2007;8:1217–1226.
37. **Lydon JP, DeMayo FJ, Funk CR, et al.** Mice lacking progesterone receptor exhibit pleiotropic reproductive abnormalities. *Genes Dev*. 1995;9:2266–2278.
38. **Shindo T, Kurihara H, Kuno K, et al.** ADAMTS-1: a metalloproteinase-disintegrin essential for normal growth, fertility, and organ morphology and function. *J Clin Invest*. 2000;105:1345–1352.
39. **Ochsner SA, Day AJ, Rugg MS, Breyer RM, Gomer RH, Richards JS.** Disrupted function of tumor necrosis factor-α-stimulated gene 6 blocks cumulus cell-oocyte complex expansion. *Endocrinology*. 2003;144:4376–4384.
40. **Russell DL, Doyle KM, Ochsner SA, Sandy JD, Richards JS.** Processing and localization of ADAMTS-1 and proteolytic cleavage of versican during cumulus matrix expansion and ovulation. *J Biol Chem*. 2003;278:42330–42339.
41. **Wisniewski HG, Vilek J.** Cytokine-induced gene expression at the crossroads of innate immunity, inflammation and fertility: TSG-6 and PTX3/TSG-14. *Cytokine Growth Factor Rev*. 2004;15:129–146.
42. **Maina V, Cotena A, Doni A, et al.** Coregulation in human leukocytes of the long pentraxin PTX3 and TSG-6. *J Leukoc Biol*. 2009;86:123–132.
43. **Fülöp C, Salustri A, Hascall VC.** Coding sequence of a hyaluronan synthase homologue expressed during expansion of the mouse cumulus-oocyte complex. *Arch Biochem Biophys*. 1997;337:261–266.
44. **Richards JS, Russell DL, Ochsner S, et al.** Novel signaling pathways that control ovarian follicular development, ovulation, and luteinization. *Recent Progr Horm Res*. 2002;57:195–220.
45. **Coukos G, Benencia F, Buckanovich RJ, Conejo-Garcia JR.** The role of dendritic cell precursors in tumour vasculogenesis. *Br J Cancer*. 2005;92:1182–1187.
46. **Dafni H, Israely T, Bhujwalla ZM, Benjamin LE, Neeman M.** Overexpression of vascular endothelial growth factor 165 drives peritumor interstitial convection and induces lymphatic drain: magnetic resonance imaging, confocal microscopy, and histological tracking of triple-labeled albumin. *Cancer Res*. 2002;62:6731–6739.
47. **Brown HM, Dunning KR, Robker RL, Pritchard M, Russell DL.** Requirement for ADAMTS-1 in extracellular matrix remodeling during ovarian folliculogenesis and lymphangiogenesis. *Dev Biol*. 2006;300:699–709.
48. **Kukk E, Lymboussaki A, Taira S, et al.** VEGF-C receptor binding and pattern of expression with VEGFR-3 suggests a role in lymphatic vascular development. *Development*. 1996;122:3829–3837.
49. **Lee L, Asada H, Kizuka F, et al.** Changes in histone modification and DNA methylation of the StAR and Cyp19a1 promoter regions in granulosa cells undergoing luteinization during ovulation in rats. *Endocrinology*. 2013;154:458–470.
50. **Andric N, Thomas M, Ascoli M.** Transactivation of the epidermal growth factor receptor is involved in the lutropin receptor-mediated down-regulation of ovarian aromatase expression in vivo. *Mol Endocrinol*. 2010;24:552–560.
51. **Norman RJ, Brannstrom M.** White cells and the ovary—incidental invaders or essential effectors? *J Endocrinol*. 1994;140:333–336.
52. **Brannstrom M, Pascoe V, Norman RJ, McClure N.** Localization of leukocyte subsets in the follicle wall and in the corpus luteum throughout the human menstrual cycle. *Fertil Steril*. 1994;61:488–495.
53. **Brännström M, Enskog A.** Leukocyte networks and ovulation. *J Reprod Immunol*. 2002;57:47–60.
54. **Fainaru O, Hantisteanu S, Rotfarb N, Michaeli M, Hallak M, Ellenbogen A.** $CD11c^+HLADR^+$ dendritic cells are present in human ovarian follicular fluid, and their maturity correlates with serum estradiol levels in response to gonadotropins. *Fertil Steril*. 2012;97:702–706.
55. **Brännström M, Mayrhofer G, Robertson SA.** Localization of leukocyte subsets in the rat ovary during the periovulatory period. *Biol Reprod*. 1993;48:277–286.
56. **Turner EC, Hughes J, Wilson H, et al.** Conditional ablation of macrophages disrupts ovarian vasculature. *Reproduction*. 2011;141:821–831.
57. **Van der Hoek KH, Maddocks S, Woodhouse CM, van Rooijen N, Robertson SA, Norman RJ.** Intrabursal injection of clodronate liposomes causes macrophage depletion and inhibits ovulation in the mouse ovary. *Biol Reprod*. 2000;62:1059–1066.
58. **Chun SY, Daphna-Iken D, Calman D, Tsafriri A.** Severe leukocyte depletion does not affect follicular rupture in the rat. *Biol Reprod*. 1993;48:905–909.
59. **Brännström M, Bonello N, Norman RJ, Robertson SA.** Reduction of ovulation rate in the rat by administration of a neutrophil-de-

pleting monoclonal antibody. *J Reprod Immunol*. 1995;29:265–270.
60. **Lucas M, Schachterle W, Oberle K, Aichele P, Diefenbach A.** Dendritic cells prime natural killer cells by trans-presenting interleukin 15. *Immunity*. 2007;26:503–517.
61. **Robker RL, Richards JS, eds.** Progesterone: lessons from the progesterone receptor knockout. In *Ovulation: Evolving Scientific and Clinical Concepts*. New York: Springer-Verlag; 2000:121–129.
62. **Hibbert ML, Stouffer RL, Wolf DP, Zelinski-Wooten MB.** Mid-cycle administration of a progesterone synthesis inhibitor prevents ovulation in primates. *Proc Natl Acad Sci USA*. 1996;93:1897–1901.
63. **Mori T, Suzuki A, Nishimura T, Kambegawa A.** Inhibition of ovulation in immature rats by anti-progesterone antiserum. *J Endocrinol*. 1977;73:185–186.
64. **Robker RL, Akison LK, Russell DL.** Control of oocyte release by progesterone receptor-regulated gene expression. *Nucl Recept Signal*. 2009;7:e012.
65. **Shozu M.** ADAMTS-1 is involved in normal follicular development, ovulatory process and organization of the medullary vascular network in the ovary. *J Mol Endocrinol*. 2005;35:343–355.
66. **Richards JS, Hernandez-Gonzalez I, Gonzalez-Robayna I, et al.** Regulated expression of ADAMTS family members in follicles and cumulus oocyte complexes: evidence for specific and redundant patterns during ovulation. *Biol Reprod*. 2005;72:1241–1255.
67. **Mittaz L, Russell DL, Wilson T, et al.** Adamts-1 is essential for the development and function of the urogenital system. *Biol Reprod*. 2004;70:1096–1105.
68. **Yoshioka S, Ochsner S, Russell DL, et al.** Expression of tumor necrosis factor-stimulated gene-6 in the rat ovary in response to an ovulatory dose of gonadotropin. *Endocrinology*. 2000;141:4114–4119.
69. **Russell DL, Ochsner SA, Hsieh M, Mulders S, Richards JS.** Hormone-regulated expression and localization of versican in the rodent ovary. *Endocrinology*. 2003;144:1020–1031.
70. **Richards JS.** Ovulation: new factors that prepare the oocyte for fertilization. *Mol Cell Endocrinol*. 2005;234:75–79.
71. **Joyce IM, Pendola FL, O'Brien M, Eppig JJ.** Regulation of prostaglandin-endoperoxide synthase 2 messenger ribonucleic acid expression in mouse granulosa cells during ovulation. *Endocrinology*. 2001;142:3187–3197.
72. **Gräs S, Hannibal J, Fahrenkrug J.** Pituitary adenylate cyclase-activating polypeptide is an auto/paracrine stimulator of acute progesterone accumulation and subsequent luteinization in cultured periovulatory granulosa/lutein cells. *Endocrinology*. 1999;140:2199–2205.
73. **Espey LL, Richards JS.** Temporal and spatial patterns of ovarian gene transcription following an ovulatory dose of gonadotropin in the rat. *Biol Reprod*. 2002;67:1662–1670.
74. **Balkwill F.** Tumour necrosis factor and cancer. *Nat Rev Cancer*. 2009;9:361–371.
75. **Takamura M, Osuga Y, Izumi G, et al.** Interleukin-17A is present in neutrophils in endometrioma and stimulates the secretion of growth-regulated oncogene-α (Gro-α) from endometrioma stromal cells. *Fertil Steril*. 2012;98:1218–1224.e1–2.
76. **Curiel TJ, Cheng P, Mottram P, et al.** Dendritic cell subsets differentially regulate angiogenesis in human ovarian cancer. *Cancer Res*. 2004;64:5535–5538.
77. **Sprague L, Muccioli M, Pate M, et al.** The interplay between surfaces and soluble factors define the immunologic and angiogenic properties of myeloid dendritic cells. *BMC Immunol*. 2011;12:35.
78. **Conejo-Garcia JR, Benencia F, Courreges MC, et al.** Tumor-infiltrating dendritic cell precursors recruited by a beta-defensin contribute to vasculogenesis under the influence of Vegf-A. *Nat Med*. 2004;10:950–958.
79. **Speyer CL, Ward PA.** Role of endothelial chemokines and their receptors during inflammation. *J Invest Surg*. 2011;24:18–27.
80. **Oliver G, Detmar M.** The rediscovery of the lymphatic system: old and new insights into the development and biological function of the lymphatic vasculature. *Genes Dev*. 2002;16:773–783.
81. **Angeli V, Randolph GJ.** Inflammation, lymphatic function, and dendritic cell migration. *Lymphat Res Biol*. 2006;4:217–228.
82. **Brown HM, Robker RL, Russell DL.** Development and hormonal regulation of the ovarian lymphatic vasculature. *Endocrinology*. 2010;151:5446–5455.
83. **Stocco DM, Wang X, Jo Y, Manna PR.** Multiple signaling pathways regulating steroidogenesis and steroidogenic acute regulatory protein expression: more complicated than we thought. *Mol Endocrinol*. 2005;19:2647–2659.